Development 135, 3071-3079 (2008) doi:10.1242/dev.022343

# Multiple *Notch* signaling events control *Drosophila* CNS midline neurogenesis, gliogenesis and neuronal identity

**Scott R. Wheeler, Stephanie B. Stagg and Stephen T. Crews***

The study of how transcriptional control and cell signaling influence neurons and glia to acquire their differentiated properties is fundamental to understanding CNS development and function. The *Drosophila* CNS midline cells are an excellent system for studying these issues because they consist of a small population of diverse cells with well-defined gene expression profiles. In this paper, the origins and differentiation of midline neurons and glia were analyzed. Midline precursor (MP) cells each divide once giving rise to two neurons; here, we use a combination of single-cell gene expression mapping and time-lapse imaging to identify individual MPs, their locations, movements and stereotyped patterns of division. The role of *Notch* signaling was investigated by analyzing 37 midline-expressed genes in *Notch* pathway mutant and misexpression embryos. *Notch* signaling had opposing functions: it inhibited neurogenesis in MP1,3,4 and promoted neurogenesis in MP5,6. *Notch* signaling also promoted midline glial and median neuroblast cell fate. This latter result suggests that the median neuroblast resembles brain neuroblasts that require *Notch* signaling, rather than nerve cord neuroblasts, the formation of which is inhibited by *Notch* signaling. Asymmetric MP daughter cell fates also depend on *Notch* signaling. One member of each pair of MP3-6 daughter cells was responsive to *Notch* signaling. By contrast, the other daughter cell asymmetrically acquired Numb, which inhibited *Notch* signaling, leading to a different fate choice. In summary, this paper describes the formation and division of MPs and multiple roles for *Notch* signaling in midline cell development, providing a foundation for comprehensive molecular analyses.

**KEY WORDS: CNS midline, *Drosophila*, Glia, Neuroblast, Neuron, *Notch***

## INTRODUCTION

The central nervous system (CNS) consists of a diverse collection of neurons and glia that differ in both morphology and function. These properties arise during a sequence of developmental events that require numerous gene regulatory and signaling processes. The cells that lie along the midline of the *Drosophila* CNS provide a useful system for the comprehensive study of neurogenesis and gliogenesis. The mature, embryonic CNS midline cells consist of a functionally diverse group of ~22 cells, including midline glia (MG), local interneurons, projection neurons, peptidergic motoneurons and neuromodulatory motoneurons (Wheeler et al., 2006). The embryonic expression patterns of nearly 300 midline-expressed genes have been identified (Kearney et al., 2004), and transcriptional maps permit detailed genetic analysis of the entire process of midline cell development (Bossing and Brand, 2006; Wheeler et al., 2006). Thus, the *Drosophila* midline cells combine cellular diversity with extensive molecular genetic characterization for the study of CNS development.

The *Drosophila* midline cells originate from about eight precursor cells/segment that undergo synchronous cell division ($\delta_{14}14$) at stage 8 (Foe, 1989) to give rise to ~16 cells (Bossing and Technau, 1994). These cells are characterized by expression of the *single-minded* (*sim*) gene (Crews, 2003; Thomas et al., 1988). By late stage 11, the midline cells consist of about ten MG, comprising two populations, the anterior midline glia (AMG) and posterior midline glia (PMG), two midline precursor 1 (MP1) neurons, two MP3 neurons, six ventral unpaired median (VUM) neurons (two VUM4s, two VUM5s and two VUM6s) and the median neuroblast (MNB) (Wheeler et al., 2006). The PMG die during embryogenesis along with about half of the AMG. The remaining three AMG ensheathe the axon commissures. Whereas the two MP1 neurons appear to be identical, the MP3 neurons differentiate into the dopaminergic H-cell and glutamatergic H-cell sib. Each VUM precursor (MP4-6) divides once, giving rise to a GABAergic VUM interneuron (iVUM4-6) and a glutamatergic/octopaminergic VUM motoneuron (mVUM4-6). Thus, MPs can give rise to either two identical neurons (MP1) or two non-identical neurons (MP3-6). The MNB stem cell divides asymmetrically to generate about eight GABAergic neurons during embryogenesis, and a much larger number postembryonically (Truman et al., 2004). Despite the small number of embryonic midline cells, the origins of midline neurons and glia remain largely unknown. In this study, for the first time, we identified each MP and described their patterns of cell division. This information was then utilized to reveal multiple roles of *Notch* signaling in midline neuronal and glial cell development.

Department of Biochemistry and Biophysics and Department of Biology, Program in Molecular Biology and Biotechnology, The University of North Carolina at Chapel Hill, Chapel Hill, NC 27599-3280, USA.

*Author for correspondence (e-mail: steve_crews@unc.edu)

**Accepted 10 July 2008**

## MATERIALS AND METHODS

### *Drosophila* strains and genetics

*Drosophila* strains included $w^{1118}$ (used as wild type), $Dl^{3}$, $Dl^{7}$, $numb^{2}$ (Uemura et al., 1989), $numb^{4}$ (Skeath and Doe, 1998), $spdo^{G104}$ and $spdo^{Z143}$ (Skeath and Doe, 1998), $N^{55e11}$, $N^{ts1}$, *P[12xSu(H)bs-lacZ]* (Go et al., 1998) and *Gbe-lacZ* (Furriols and Bray, 2001). *Gal4* and *UAS* lines used were: *sim-Gal4* (Xiao et al., 1996), *UAS-numb* (Wang et al., 1997), *UAS-spdo* (O'Connor-Giles and Skeath, 2003), *UAS-Su(H).VP16* (Kidd et al., 1998) and *UAS-tau-GFP* (Brand, 1995). For *N* temperature-shift experiments, $N^{55e11}/N^{ts1}$ embryos were collected for 2 hours at 18°C, further incubated for 2 hours at 18°, then shifted to the restrictive temperature (30°C) for 6 hours, followed by fixation (approximately stage 14).

### In situ hybridization and immunostaining

Embryo collection, in situ hybridization and immunostaining were performed as previously described (Kearney et al., 2004). Primary antibodies used were: mouse (Promega) and rabbit (Cappel) anti-β-galactosidase, rabbit anti-Cas

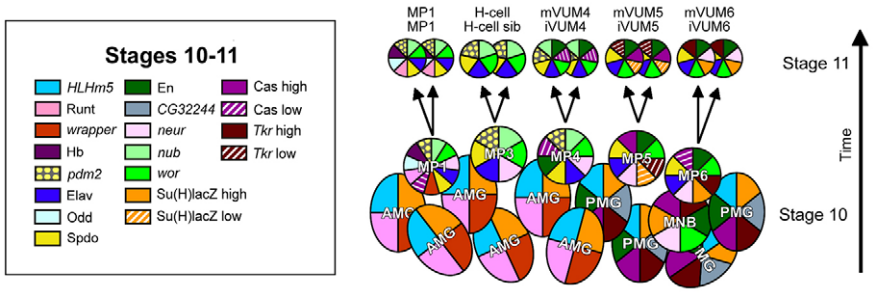


**Fig. 1. Formation of midline precursors (MPs) and MP neurons in *Drosophila*.** Molecular map of stage 10 and 11 MPs and midline neurons (circles) and glia (ovals) shown in sagittal view. One segment is shown, with anterior to the left and interior (basal) at top. Each cell is depicted in terms of its pattern of gene expression as indicated by colors (the corresponding genes as listed on the left). The five MPs are shown at late stage 10, and the arrows indicate MPs dividing into their neuronal progeny at stage 11. The number of midline glia does not change appreciably from stage 10 to 11.

(Kambadur et al., 1998), mouse and rat anti-Elav [Developmental Studies Hybridoma Bank (DSHB)], mouse anti-En MAb 4D9 (Patel et al., 1989), anti-Futsch MAb 22C10 (DSHB), guinea pig anti-Hb [East Asian Distribution Center (EADC)] (Kosman et al., 1998), chicken anti-GFP (Upstate), rabbit anti-GFP (Abcam), guinea pig anti-Lim1 (Broihier and Skeath, 2002), guinea pig anti-Numb (O'Connor-Giles and Skeath, 2003), rabbit anti-Odd (Ward and Skeath, 2000), rabbit anti-Period (Per) (Liu et al., 1992), rabbit anti-phosphohistone H3 (Millipore), guinea pig anti-Runt (EADC), guinea pig and rat anti-Sim (Ward et al., 1998), rabbit anti-Spdo (O'Connor-Giles and Skeath, 2003), mouse anti-Tau (Sigma) and rat anti-Tup (Broihier and Skeath, 2002). Alexa Fluor-conjugated secondary antibodies were used (Molecular Probes). The Tyramide Signal Amplification System (Perkin Elmer) was employed for some immunostaining.

### Microscopy and image analysis

In situ hybridization and immunostaining were carried out as previously described (Kearney et al., 2004; Wheeler et al., 2006). Midline cells were examined in abdominal segments A1-8. Owing to the three-dimensional structure of the midline cells, it was difficult to represent all relevant cells in a single focal plane, so, for clarity, irrelevant portions of single images within a stack of confocal images were subtracted and projections were generated. Thus, a single composite image is made from different focal planes that each contained relevant data.

### Live imaging of midline cells

Time-lapse imaging of midline cell development was carried out in *sim-Gal4 UAS-tau-GFP* and *sim-Gal4 UAS-tau-GFP*; $Dl^3/Dl^3$ embryos by visualizing GFP. Embryos were collected for 1 hour, aged for an additional 4 hours, dechorionated, mounted on a glass coverslip, and immersed in halocarbon oil 700 on slides containing an oxygen-permeable membrane. GFP-fluorescent images were captured using a Nikon Eclipse TE300 equipped with a Perkin Elmer Ultraview confocal scanner and 40× or 60× oil-immersion objectives. Embryos were visualized for ~4 hours with an image captured every 30 seconds. Movies were assembled from images of single focal planes using MetaMorph software (Molecular Devices). Ten movies of wild-type embryos viewing 29 segments, and five movies of *Dl* mutant embryos viewing 14 distinct groups of cells, were analyzed.

## RESULTS

## Identification of midline precursors and their pattern of division

As a prelude to studying the molecular mechanisms that control MP neuronal cell fate decisions, it was important to identify the MPs and to determine when these cells divide. Previously, we generated molecular maps of stages 9, late 11, 13 and 17 (Wheeler et al., 2006), which allowed identification of individual midline cells. In this paper, we mapped the midline cell expression of 16 genes (Fig. 1 and see Fig. S1 in the supplementary material) at multiple periods during stages 10-11 of embryogenesis. Each of the MPs, the MNB, and their progeny, were defined and distinguished from each other by gene expression differences, position, size and visualization of cell division. These data provided strong evidence that MP divisions occur during stage 11, as confirmed by time-lapse imaging of midline cells in *sim-Gal4 UAS-tau-GFP* embryos (Fig. 2 and see Movie 1 in the supplementary material).

At early stage 10, the midline cells constitute a monolayer along the anterior-posterior axis. However, beginning at late stage 10, MPs began to delaminate, and migrated basally (internally). As the cells migrated, they retracted a cytoplasmic process from the apical surface. The MP1,3,4 precursors acquired a flattened shape, resided internal to the MG, and were separated from other MPs by MG. The five MPs were arranged in a defined order, MP1→MP3→MP4→MP5→MP6 (anterior to posterior), within the segment. However, they delaminated and divided in the order MP4→MP3→MP5→MP1→MP6. The MP divisions were characterized by loss of an apical projection, retraction of the MG that separate the MPs, and the subsequent juxtaposition of neuronal progeny. The MP3-6 divisions were along the apical-basal axis, whereas the MP1 division was perpendicular to the apical-basal axis. After the MPs divided, the MNB delaminated posterior to the MP6 progeny and began dividing to generate ganglion mother cells (GMCs).

## *Notch* signaling promotes midline glia, MNB and MP5,6 formation and inhibits MP1,3,4 formation

Based on the important roles of *Notch* signaling in CNS development, *Delta* (*Dl*) and *Notch* (*N*) mutants were screened for midline phenotypes, including alterations in expression of midline-expressed genes. In both $Dl^3$ homozygotes and $Dl^3/Dl^7$ transheterozygotes, an increase was observed in the number of midline neurons at the expense of MG (Fig. 3). At stage 14, the number of MP1 neurons increased from two cells/segment to 9.3±1.6 ($n$=14 segments) cells (Fig. 3A,F). The number of H-cells increased from one cell/segment to 9.6±1.1 ($n$=17) (Fig. 3B,G), and the number of mVUMs increased from three cells/segment to 11.5±1.7 ($n$=51) (Fig. 3C,H). H-cell sib- and iVUM-specific gene expression was absent in *Dl* mutants (not shown). As described below, in the absence of *Notch* signaling, all MP3 neurons are H-cells and all VUMs are mVUMs owing to cell fate defects. Both MP1 and MP3 neurons increased ~5-fold in *Dl* mutant embryos. The VUM neurons, by contrast, increased only 2-fold.

This disparity led us to investigate the identity of the mVUM neurons observed in *Dl* mutants. All mVUMs can be uniquely identified in the midline by *Tyramine β hydroxylase* (*Tbh*) expression, and mVUM4-6 can be distinguished from each other based on *Tyrosine kinase-related protein* (*Tkr*) and Castor (Cas) levels. The wild-type mVUM4 and mVUM5 neurons are $Tkr^-$, whereas mVUM6 is $Tkr^+$ (Fig. 4A). The expanded $Tbh^+$ mVUMs in *Dl* mutants were $Tkr^-$ (Fig. 4C), indicating that none was mVUM6. The one significant difference between wild-type mVUM4 and mVUM5 is that mVUM4 has low levels of Cas ($Cas^{lo}$) and mVUM5 has high levels of Cas ($Cas^{hi}$) (Fig. 4B). Quantitation

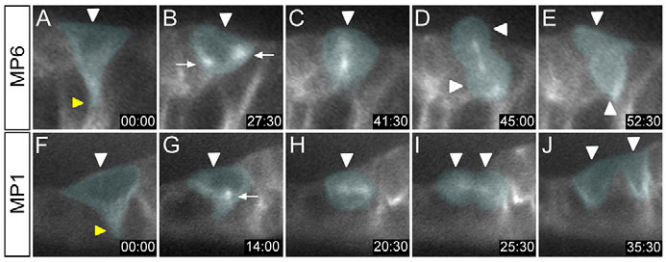


**Fig. 2. Time-lapse imaging of sequential MP delamination and division.** Images in sagittal view, internal (basal) up, from time-lapse imaging of an (A-E) MP6 division and an (F-J) MP1 division. GFP fluorescence was visualized in *sim-Gal4 UAS tau-GFP* embryos during stage 11. Time is displayed as minutes:seconds. Relevant cells in each panel are pseudocolored. (**A**) Prior to division, the MP6 (white arrowhead) delaminates from the apical surface and takes on a triangular shape. The tip of the retracting cell is indicated by the yellow arrowhead. (**B-D**) During mitosis, (B) the centrosomes (arrows) move toward opposite poles, (C) the spindle fibers have an apical-basal orientation, and (D) the MP6 divides (arrowheads) along this axis. (**E**) Two MP6 neurons (arrowheads) are produced. (**F**) The MP1 (white arrowhead) delaminates from the apical surface, also acquiring a triangular shape (retraction point, yellow arrowhead). (**G**) The centrosomes (arrow) can be seen just before they separate and begin their migration. (**H**) The MP1 spindle maintains an orientation perpendicular to the apical-basal axis. (**I**,**J**) Cytokinesis results in the formation of two MP1 neurons (arrowheads).

of Cas staining intensity was measured using the Mean Gray Value (MGV) function of ImageJ (Abramoff et al., 2004). In wild type ($n$=4 segments), mVUM4, mVUM5 and mVUM6 showed MGVs of 67, 155 and 22, respectively. In *Dl* mutants ($n$=6 segments), all *Tbh*$^+$ cells showed similar MGVs with an average of 67, identifying them as mVUM4s. These results, together with the observation that the 11.5 mVUMs/segment observed in *Dl* mutants was close in number to the approximately nine MP1s and ten H-cells observed, suggested an expansion of a single VUM precursor, probably the MP4.

The expanded numbers of MP1,3,4 neurons in *Dl* mutant embryos (~30) could be due to either: (1) a transformation of all of the ~16 midline cells to MPs1,3,4, followed by a single division of each MP; or (2) an overproliferation of one or a few MP1,3,4 cells, accompanied by the death or unrecognizable fate change of the other midline cells. This was tested by assaying stage 10-11 *Dl* mutant embryos for gene expression and positions and timing of cell division. Late stage 10 mutant embryos had an increased number of Odd-skipped (Odd)$^+$ MP1s (4.1±1.2; $n$=17) (Fig. 4E,F). Live imaging of *Dl* mutant embryos during stage 11 indicated that the observable MP divisions occurred within a relatively short time interval (88±16 minutes) (see Movie 2 in the supplementary material). Divisions of closely juxtaposed cells were frequently observed to occur in close temporal sequence in both live imaging and fixed embryos stained for phosphohistone H3 (Fig. 4G). There was no evidence of cell death. Confocal imaging of stage 11 *Dl* embryos, after division, revealed 7.9±2.1 ($n$=19) Odd$^+$ Cas$^+$ MP1 neurons, 6.9±1.4 ($n$=12) Odd$^-$ Cas$^-$ MP3 neurons, and 10.0±2.2 ($n$=7) Odd$^-$ Cas$^+$ MP4s (Fig. 4H). These data are most consistent with a model in which there is a transformation of ~16 midline cells into approximately five MP1s, five MP3s and six MP4s, followed by a single division of each MP.

In contrast to the expansion of MP1,3,4-derived neurons in *Dl* mutants, there was an absence of MG and of the MNB. MG gene expression was reduced from 10.0±1.3 ($n$=15) cells/segment in the wild type to 0.1±0.2 ($n$=176) cells/segment in *Dl* mutants (Fig. 3E,J). The wild-type MNB has prominent expression of three genes: *worniu* (*wor*) (Fig. 3D), *miranda* (*mira*) (not shown), and *sanpodo* (*spdo*) (not shown), which are specific to the MNB after stage 11. In

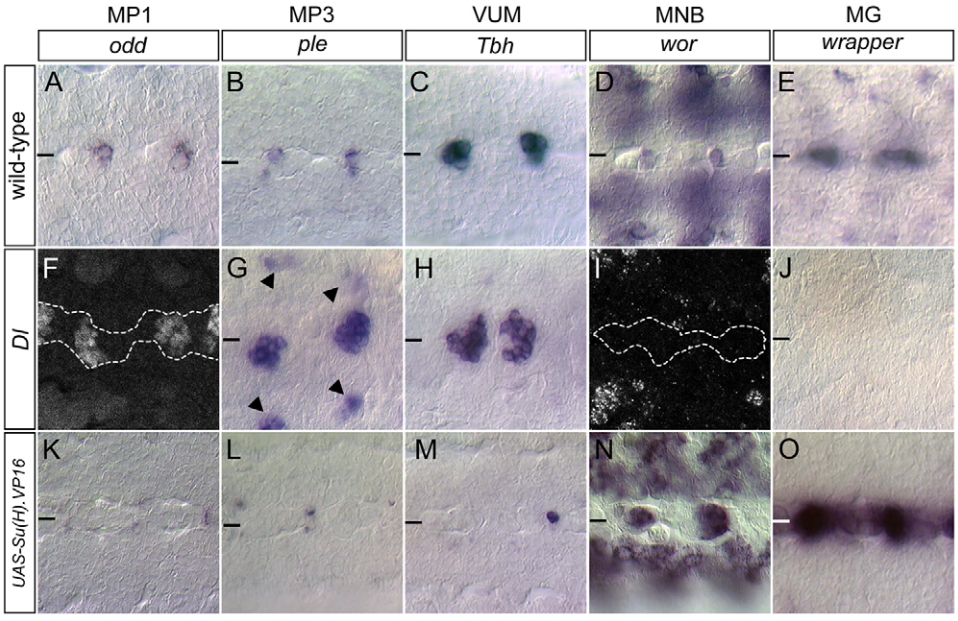


**Fig. 3. *Notch* signaling influences midline cell fate.** Ventral views of (**A-E**) wild-type, (**F**,**G**,**I**,**J**) $Dl^3/Dl^3$, (**H**) $Dl^3/Dl^7$ and (**K-O**) *sim-Gal4 UAS-Su(H).VP16* stage 14 *Drosophila* embryos. Cell types are listed at the top of each column, and the gene or protein assayed that identifies each cell type is listed below. Horizontal bars indicate the location of the midline. (F,I) To differentiate (F) Odd$^+$ and (I) *wor*$^+$ midline cells from lateral CNS cells, embryos were double-stained with anti-Sim [not shown, but outlined (dashed line) to show location of midline cells]. In *Dl* mutants, there was an (F-H) increase in MP1, MP3 (H-cell) and mVUM neurons, and an absence of the (I) MNB and (J) MG. (G) Ectopic *ple*$^+$ cells (arrowheads) were present off the midline; double-staining with anti-Sim indicated that these are not midline-derived (not shown). (K-O) *sim-Gal4 UAS-Su(H).VP16* embryos showed the opposite phenotype to *Dl* mutants: (K-M) strong reduction of MP1, MP3 and mVUM neurons, and increases in (N) MNB and (O) MG.

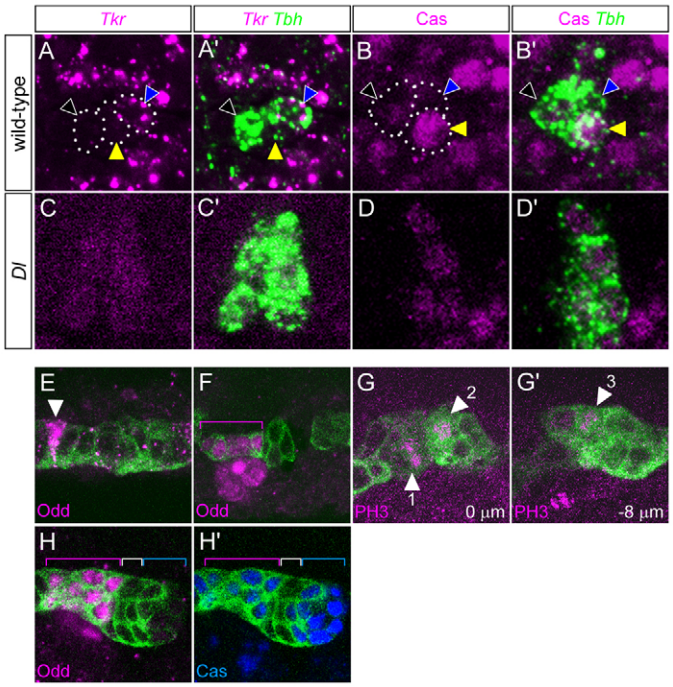


**Fig. 4. MP number increases in the absence of *Notch* signaling.** (**A-D**′) Ventral views of (A-B′) wild-type and (C-D′) $Dl^3/Dl^3$ mutant stage 14 *Drosophila* embryos. (A,A′,C,C′) Single segments stained for *Tkr* (magenta) and *Tbh* (green). (A,A′) The mVUM6 (blue arrowhead) was $Tkr^+$, whereas mVUM4 (black arrowhead) and mVUM5 (yellow arrowhead) were $Tkr^-$. Dotted ovals outline the mVUMs. (C,C′) In *Dl*, *Tkr* expression was absent indicating that the excess $Tbh^+$ cells were not mVUM6s. (B,B′,D,D′) Single segments stained for Cas (magenta) and *Tbh* (green). (B,B′) There are three $Tbh^+$ mVUMs in each segment: mVUM4 (black arrowhead) was $Cas^{lo}$, mVUM5 (yellow arrowhead) was $Cas^{hi}$, and mVUM6 was $Cas^-$ (blue arrowhead). (D,D′) Excess $Tbh^+$ cells in *Dl* mutants were $Cas^{lo}$, indicating that they were mVUM4s. (**E-H**′) Sagittal views of single segments of (E) wild-type and (F-H′) $Dl^3/Dl^3$ mutant embryos. Midline cells are defined as MPs based on their presence at stage 10 and relatively large size. (E) At mid-stage 10, there is a single $Odd^+$ (magenta) MP1 (arrowhead). (F) In *Dl*, the number of $Odd^+$ MP1s (bracket) was increased. (G,G′) *Dl* mutant embryo at two focal planes, 8 µm apart, showing three dividing cells (arrowheads 1-3) in close proximity, stained with anti-phosphohistone H3 (PH3, magenta). (H,H′) In *Dl*, there is an increase in $Odd^+$ (magenta) $Cas^+$ (blue) MP1 neurons (magenta bracket), $Odd^-$ $Cas^-$ MP3 neurons (white bracket), and $Odd^-$ $Cas^+$ MP4 neurons (blue bracket).

stage 14 *Dl* mutant embryos, *wor* (*n*=84) (Fig. 3I), *mira* (*n*=56) and *spdo* (*n*=47) expression was absent from the midline. Involvement of the Notch receptor was confirmed by analysis of a *N* mutant combination, $N^{ts1}/N^{55e11}$, that showed similar phenotypes to *Dl* mutants, although at a reduced frequency (not shown).

## *Notch* activation converts MPs to midline glia

In experiments complementary to *Notch* and *Dl* mutant analyses, *sim-Gal4* was used to misexpress constitutively-active *Suppressor of Hairless.VP16* [*Su(H).VP16*] (Kidd et al., 1998) in all midline cells. Stage 14 *sim-Gal4 UAS-Su(H).VP16* embryos were examined because MG undergo apoptosis beginning at stage 15. At stage 14, these embryos showed a 3-fold increase in the number of MG (30±5.5 cells/segment, *n*=19) compared with wild type (10.0±1.3, *n*=15) (Fig. 3E,O, and see Fig. S2A-H in the supplementary material). The expanded MG had wild-type properties: they underwent apoptosis, both AMG and PMG were present, and they wrapped commissural axons. In addition, there was a near complete absence of midline axons (see Fig. S3A,B in the supplementary material) and fewer than one MP-derived neuron/segment was present (Fig. 3K-M). The larval and adult phenotypes of these midline neuron-less animals were assessed: 62% of embryos survived to adulthood, but were female sterile (see Fig. S3C in the supplementary material), and larvae had reduced motility (see Fig. S3D in the supplementary material). When *sim-Gal4 UAS-Su(H).VP16* embryos were stained for the MNB markers *wor* (Fig. 3N), *mira* and *spdo*, there was an increase in cell number from one cell/segment in the wild type to 4.9±1.8 (*n*=12). These $wor^+$ cells also had MG gene expression. The expansion of MNB gene expression was consistent with the *Dl* mutant data indicating that *Notch* signaling was required for MNB formation. By contrast, there was no evidence that *Su(H).VP16* misexpression resulted in additional MP5,6 progeny.

To further understand the spatial and temporal dynamics of midline *Notch* signaling, the expression of two reporters of *Su(H)* activity was examined: *P[12xSu(H)bs-lacZ]* (Go et al., 1998) and *Gbe-lacZ* (Furriols and Bray, 2001). Reporter expression was observed in AMG and PMG during stage 10, and was maintained through to the end of embryogenesis, although levels were low by stage 17 (see Fig. S2I-L in the supplementary material). Expression was dependent on *Notch* signaling, as it was absent in the CNS midline cells in *Dl* mutant embryos (see Fig. S2M,N in the supplementary material). In addition to MG, expression of *P[12xSu(H)bs-lacZ]* was present in MP5,6 and in the MNB (see Fig. S2I-K in the supplementary material) during stage 11, prior to their division. MP5 expresses a low level of *P[12xSu(H)bs-lacZ]*, MP6 an intermediate level, and the MNB higher levels. After division, the MP5,6 and MNB progeny express *P[12xSu(H)bs-lacZ]* at the same relative levels as the precursors (see Fig. S2L in the supplementary material). The neuronal expression is maintained throughout embryogenesis. No expression of the reporter was observed in MP1,3,4 or their progeny. The expression pattern of *Gbe-lacZ* was similar, although levels of *lacZ* expression were reduced compared with *P[12xSu(H)bs-lacZ]*. These data indicate that *Notch* signaling is occurring in MG, MP5, MP6 and the MNB during stages 10-11, consistent with genetic requirements for *Notch* signaling in these cells.

## *numb* and *spdo* direct sibling neuronal fates in MP asymmetric divisions

MPs either divide symmetrically (MP1) or asymmetrically (MP3-6). A possible mechanism for generating MP asymmetric cell fates is asymmetric localization of Numb in conjunction with *Notch* signaling. To assess cell fate in *Dl*, *numb* and *spdo* mutant and overexpression embryos, the MP1, MP3 and VUM neurons were analyzed for changes in the expression of 37 genes, which encode transcription factors, signaling molecules, neurotransmitter biosynthetic enzymes, neurotransmitter receptors and neuropeptide receptors. Additionally, axonal trajectories were analyzed based on *sim-Gal4 UAS-tauGFP* visualization.

### MP3 neurons

Analysis of 19 genes expressed in the H-cell and H-cell sib neurons showed that H-cell-specific gene expression was absent in *numb* mutant embryos (Fig. 5A,B,F,G), but was present in both neurons in *spdo* mutants (Fig. 5K,L). The opposite results were observed for H-cell sib-specific gene expression (Fig. 5C,D,H,I,M,N). Another

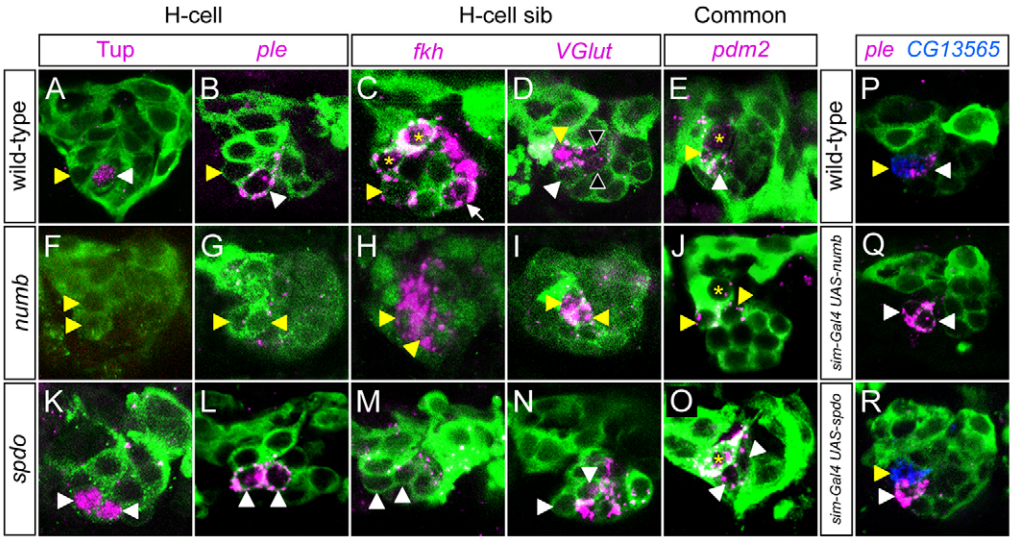


**Fig. 5. *numb* and *spdo* control MP3 neuronal cell fate.** Confocal images of stage 14-15 *Drosophila* embryos in sagittal view. (**A-E**,**P**) Wild type, (**F-J**) $numb^4/numb^4$, (**K-O**) $spdo^{G104}/spdo^{G104}$, (**Q**) *sim-Gal4 UAS-numb* and (**R**) *sim-Gal4 UAS-spdo*. All embryos had *sim-Gal4 UAS-tau-GFP* (green) in the background, except H, which shows anti-Sim (green) staining. To identify the MP3 neurons, *numb* mutants were double-labeled with *Vesicular glutamate transporter* (*VGlut*) (not shown, except in I); *spdo* mutants were double-labeled with *ple* (not shown, except in L). In A-O, white arrowheads denote cells expressing H-cell genes and yellow arrowheads indicate cells expressing H-cell sib genes. (A,B) In wild type, Tailup (Tup) protein and *ple* were present in the H-cell, and absent from H-cell sib. (F,G) In *numb*, Tup and *ple* were absent from both MP3 neurons. (K,L) In *spdo*, Tup and *ple* were present in both MP3 neurons. (C) In wild type, *fork head* (*fkh*) was expressed in H-cell sib, the two MP1 neurons (*) and iVUMs; only one iVUM (arrow) is present in this focal plane. (H) In *numb*, *fkh* was expressed in two $Sim^+$ MP3 neurons, and was absent (M) from *spdo* MP3 neurons. (D) In wild type, *VGlut* was expressed in H-cell sib and at a lower level in mVUMs (black arrowheads), whereas (I) in *numb*, *VGlut* was expressed in two MP3 neurons and absent from VUM neurons. By contrast, (N) in *spdo*, the two MP3 neurons (arrowheads) lacked *VGlut*, whereas it was present in all VUM neurons. (E) *pdm2* was expressed in the MP1 (*) neurons and in both MP3 neurons in wild type (only one MP1 neuron is present in this focal plane). The expression of *pdm2* was unaltered in (J) *numb* and (O) *spdo*. (P-R) Overexpression of *numb*, but not *spdo*, causes an MP3 cell fate change. The H-cell is marked by *ple* expression (magenta) and H-cell sib by *CG13565* expression (blue). (P) Wild-type expression of *ple* and *CG13565*. (Q) In *sim-Gal4 UAS-numb*, H-cell sib was transformed into an H-cell, as shown by the presence of two $ple^+$ cells and the absence of *CG13565*-expressing cells. (R) *sim-Gal4 UAS-spdo* showed a wild-type pattern of gene expression with a single $ple^+$ cell and a single $CG13565^+$ cell.

indicator of neuronal cell fate is axonal trajectory. Consistent with the gene expression results, *numb* mutants showed an absence of H-cell axons and the presence of H-cell sib axons, whereas *spdo* mutants showed the opposite phenotype (see Fig. S4A-C in the supplementary material). These results were confirmed by analysis of H-cell gene expression in *numb*-overexpression and *Dl* mutant embryos. When *numb* was overexpressed in all midline cells, there were two *pale* (*ple*)$^+$ cells (H-cells), an absence of $CG13565^+$ H-cell sib, and a duplication of H-cell axons (Fig. 5P,Q; see Fig. S4D in the supplementary material). Overexpression of *spdo* did not result in cell fate defects (Fig. 5R). Analysis of *Dl* mutant embryos revealed an expansion of neurons derived from the MP3. Only $ple^+$ H-cells (Fig. 3G), and not $CG13565^+$ H-cell sibs (data not shown), were present. Four genes, including *POU domain protein 2* (*pdm2*) (Fig. 5E,J,O), that are expressed in both cell types had no alterations in expression in either *numb* or *spdo* mutant embryos, indicating that *numb* and *spdo* affect cell type-specific gene expression, but not expression present in both cells. Thus, assays of both neuronal morphology and gene expression indicated that *Notch* controls all of the divergent aspects of H-cell versus H-cell sib cell fate.

### VUM neurons

The expression of 21 VUM neuron-expressed genes (see Table S1 in the supplementary material) was examined in *numb* and *spdo* mutants. mVUM-specific gene expression was absent in *numb* mutant embryos and expanded in *spdo* mutants (Fig. 6A,B,F,G,K,L). By contrast, iVUM-specific gene expression was expanded in *numb* mutants and absent from *spdo* mutants (Fig. 6C,D,H,I,M,N). In *numb* mutant embryos, the mVUM axons were absent and the iVUM axons appeared thickened, suggesting a duplication; *spdo* mutants had the opposite phenotype (see Fig. S4E-G in the supplementary material). Embryos mutant for *Dl* showed an increase in $Tbh^+$ mVUMs (Fig. 3H), but lacked $CG15236^+$ iVUMs (data not shown). In *sim-Gal4 UAS-numb* embryos, *Tbh* expression (mVUMs) was expanded to six cells and Engrailed (En) (iVUMs) was absent (Fig. 6P,Q). Furthermore, mVUM but not iVUM axons were present (see Fig. S4H in the supplementary material). Analysis of *sim-Gal4 UAS-spdo* did not show alterations in VUM cell fate (Fig. 6R). Genes expressed in both iVUMs and mVUMs showed no alterations in expression in either *numb* or *spdo* mutants (Fig. 6E,J,O). In conclusion, *Notch* signaling, in conjunction with *numb* and *spdo*, controls iVUM/mVUM asymmetric cell fate choices.

### MP1 neurons

The MP1 neurons are unique among MP progeny in that they appear identical. Consequently, their development might be independent of *numb* and *spdo* regulation. This was addressed by examining mutant and overexpression embryos for ten MP1-expressed genes (see Table S1 and Fig. S5 in the supplementary material). There were no alterations in MP1 neuronal gene expression in *numb*, *spdo* or *sim-Gal4 UAS-numb* embryos (see Fig. S5 in the supplementary material), nor were there alterations in MP1 neuronal axonal trajectories (see Fig. S5A-E,G in the supplementary material). These

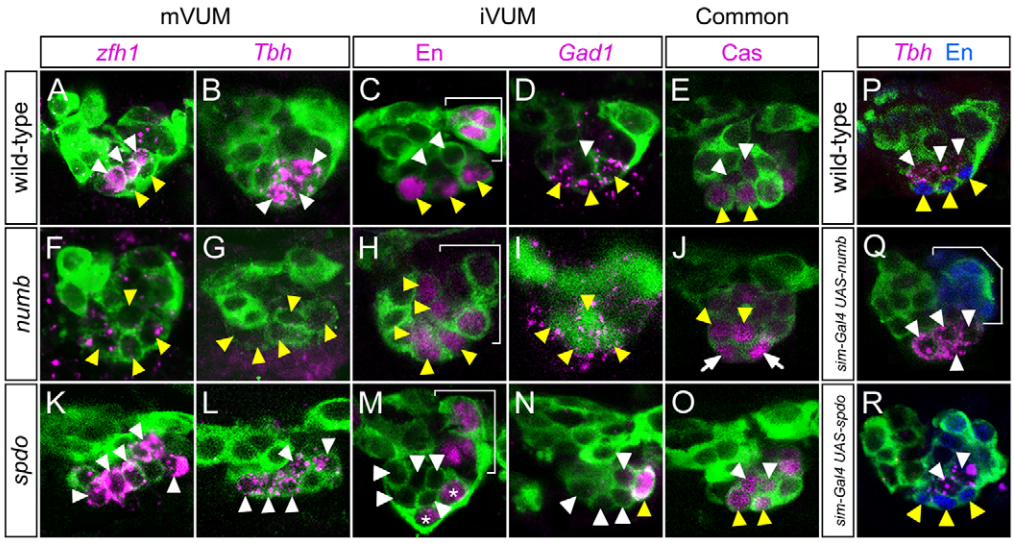


**Fig. 6. *numb* and *spdo* control VUM neuronal cell fate.** Confocal images of stage 14-15 *Drosophila* embryos in sagittal view. (**A-E**,**P**) Wild-type, (**F-J**) $numb^{4}/numb^{4}$, (**K-O**) $spdo^{G104}/spdo^{G104}$, (**Q**) *sim-Gal4 UAS-numb* and (**R**) *sim-Gal4 UAS-spdo*. All embryos had *sim-Gal4 UAS-tau-GFP* (green) in the background, except I, which shows anti-Sim (green) staining. To identify the VUM neurons, *numb* mutants were double-labeled for En (not shown, except in H); *spdo* mutants were double-labeled with *Tbh* (not shown, except in L). In A-O, white arrowheads indicate cells expressing mVUM genes and yellow arrowheads indicate cells expressing iVUM genes. (A) In wild type, *Zn finger homeodomain 1* (*zfh1*) was present in all three mVUMs and not in the iVUMs. (F) In *numb*, *zfh1* expression was absent. (K) In *spdo*, *zfh1* expression was expanded to five VUMs. (B) *Tbh* was expressed in three mVUMs in wild type. (G) In *numb*, *Tbh* was not expressed. (L) In *spdo*, five VUMs expressed *Tbh*. (C) In wild type, En was present in three iVUMs as well as other cell types, including the PMG (bracket). (H) In *numb*, En was present in five VUMs in addition to the PMG (bracket). (M) In *spdo*, En was absent from VUMs, but was present in the PMG (asterisk and bracket). (D) *Glutamic acid decarboxylase 1* (*Gad1*) was expressed in three iVUMs in wild type. (I) *Gad1* expression was expanded to six cells in *numb* (four of the six VUMs can be seen in this focal plane). (N) In *spdo*, *Gad1* expression was present in only one VUM. (E) In wild type, Cas was present in two iVUMs (iVUM4,5) and two mVUMs (mVUM4,5). In (J) *numb* and (O) *spdo* mutant embryos, Cas was also present in iVUM4,5 and mVUM4,5. (P-R) Overexpression of *numb* causes a VUM cell fate change. (P) Wild-type expression of *Tbh* (magenta) in three mVUMs and of En protein (blue) in three iVUMs. (Q) In *sim-Gal4 UAS-numb*, six ventral $Tbh^{+}$ $En^{-}$ mVUMs (two of the six cells are absent in this focal plane) were present. En in PMG (bracket) was unaffected. (R) *sim-Gal4 UAS-spdo* had a wild-type *Tbh* and En pattern (two of three $Tbh^{+}$ mVUMs are present in this image).

data indicate that *numb* and *spdo* do not play a role in the cell fate specification of MP1 neurons. In *Dl* mutant embryos, we observed an expanded set of neurons that are $Hunchback^{+}$ and $Odd^{+}$ (Fig. 3F); within the midline, these genes are specific for the MP1 neurons. Taken together, the *Dl*, *numb* and *spdo* mutant results suggest that *Notch* signaling is not important for MP1 cell fate determination.

### Numb and Spdo are localized asymmetrically during MP3-6, but not MP1, divisions

Analysis of the *numb* and *spdo* mutant phenotypes suggested that Numb and Spdo proteins would be asymmetrically localized during MP divisions. Our analysis showed that Numb localization was regulated in a cell-cycle-dependent manner in MP3-6. Prior to mitosis, Numb was localized uniformly around the MP cell membrane (Fig. 7A), then became enriched along the basolateral surface (Fig. 7B), and finally segregated into only the basal H-cell daughter (Fig. 7C,D). During mitosis (Fig. 7G-I), Spdo was localized around the MP membrane and in puncta throughout the cytoplasm. Immediately after division, Spdo was localized uniformly around the membrane of the $Numb^{-}$ daughter cell at a low level (Fig. 7J), whereas in the $Numb^{+}$ cell the membrane localization of Spdo was reduced, being instead found in intracellular puncta (Fig. 7J). These puncta are likely to be intracellular vesicles (Hutterer and Knoblich, 2005; O'Connor-Giles and Skeath, 2003). In summary, MPs asymmetrically generate a $Numb^{+}$ intracellular $Spdo^{+}$ neuron (H-cell, mVUM) and a $Numb^{-}$ cortical $Spdo^{+}$ neuron (H-cell sib, iVUM).

What happens in the MP1, which generates two identical neurons? In this case, Numb was uniformly localized to the membrane prior to, during and after MP1 cell division (Fig. 7E,F). Spdo was found at the membrane and in cytoplasmic puncta prior to and during division, and in both progeny after division (Fig. 7K,L). Although Numb is present in both MP1 neurons, other mechanisms must cause these cells to be refractory to *Notch* signaling because *numb* mutants do not exhibit changes in MP1 gene expression.

## DISCUSSION

### Patterns of stage 10-11 midline cell divisions and gene expression

The *Drosophila* MPs form at specific positions and divide in a reproducible sequence. Descriptive work in grasshopper indicated that MPs each undergo a single division (Bate and Grunewald, 1981; Goodman et al., 1981; Jia and Siegler, 2002). We propose that the *Drosophila* cells described here are homologous, and that MP4 gives rise to the anterior pair of VUMs (VUM4s), MP5 to the medial VUM pair (VUM5s), and MP6 to the posterior VUM pair (VUM6s). This picture of *Drosophila* stage 11 MP divisions runs counter to the prevailing *Drosophila* models, which propose that the MP divisions occur at stage 8 during the $\delta_{14}14$ synchronous cell division (Bossing and Technau, 1994; Jacobs, 2000; Klambt et al., 1991). Instead, we propose that the precursors dividing at stage 8 give rise to glial-glial, neuronal-neuronal and mixed glial-neuronal lineages (Fig. 8). In general, this new model fits DiI-labeling data from previous reports in which mixed clones were noted (Bossing and Technau, 1994; Schmid et al., 1999), but no compelling arguments put forward for how they arose.

### *Notch* signaling directs the formation of midline glia and inhibits neurogenesis

*Dl* mutant and *Su(H)* misexpression experiments indicated that: (1) *Notch* signaling is required for the formation of both AMG and PMG; (2) Dl is a ligand for N; and (3) transcriptional output involves Su(H) beginning at stage 10. Consistent with these results, analysis

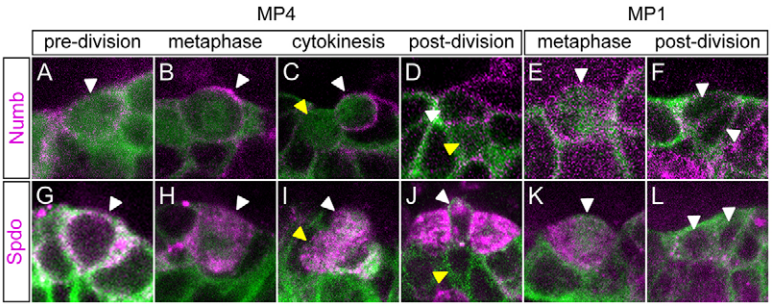


**Fig. 7. Numb and Spdo localization during MP divisions.** Confocal images of MP1 and MP4 divisions in *sim-Gal4 UAS-tau-GFP* (green) stage 11 *Drosophila* embryos stained with (**A-F**) anti-Numb (magenta) and (**G-L**) anti-Spdo (magenta). Sagittal views with anterior left and internal (basal) up. White arrowheads indicate: (A,B,G,H) MP4, (C,D) Numb$^+$ VUM4 neuron, (I,J) basal VUM4 neuron with cytoplasmic punctate Spdo, (E,K) MP1 and (F,L) MP1 neurons. Yellow arrowheads indicate: (C,D) Numb$^-$ VUM4 neuron, (I) apical VUM4 neuron with cytoplasmic punctate Spdo and (J) membranous Spdo VUM4 neuron.

of a $N^{ts}$ mutant showed changes in expression in MG and neuronal enhancer-trap lines, but lacked specific markers to fully characterize the phenotype (Menne and Klambt, 1994). Genes of the *Enhancer of split-Complex* [*E(spl)-C*] are commonly activated by *Notch* signaling and repress transcription. We note that the *HLHm5 E(spl)-C* gene is expressed specifically in MG at stages 10-11 (Fig. 1), and other *E(spl)-C* members are also expressed in midline cells (Kearney et al., 2004; Wech et al., 1999). While *E(spl)-C* genes could be direct targets of Su(H) and repress midline neuronal gene expression in MG, what activates MG gene expression? The *sim* gene was previously shown to activate MG gene transcription (Ma et al., 2000; Wharton et al., 1994), and could be a direct target of Su(H).

*Dl* mutants not only showed a complete lack of MG gene expression, but also an expansion of anterior midline neurons (MP1,3 and VUM4) and absence of posterior neurons (VUM5,6 and MNB). Expanded MP1s have also been noted in work describing the role of *Notch* signaling in MP2 development (Spana and Doe, 1996). Do the expanded *Dl* mutant MP1,3,4 neurons result from transformation of MG precursors to MPs, or from excessive division of a small number of MPs? Analysis of *Dl* mutants at stages 10-11 suggests that the midline cells at these stages consist of approximately five MP1s, five MP3s and six MP4s. If each divided once, this would equal the ten MP1 neurons, ten H-cells and 12 mVUM4s observed in *Dl* mutant embryos at later stages. In this model (Fig. 8), *Notch* signaling promotes MG development, while MP1, MP3 and MP4 are selected from their respective MP fields. This midline role for *Notch* parallels known functions of *Notch* in both *Drosophila* and vertebrates, in which it promotes gliogenesis and inhibits neurogenesis (Gaiano et al., 2000; Morrison et al., 2000; Udolph et al., 2001).

## *Notch* signaling promotes MNB and MP5,6 formation

The progeny of MP5,6 and the MNB were absent from *Dl* mutants, indicating that *Notch* signaling is required for the formation of the MNB as well as for VUM5,6. This was a surprising result for the MNB because in the ventral nerve cord, *Notch* signaling inhibits NB formation early in development (Campos-Ortega, 1993) and plays no apparent role in the asymmetric division of postembryonic nerve cord NBs (Almeida and Bray, 2005). However, *Notch* signaling controls central brain NB number (Lee et al., 2006; Wang et al., 2007), indicating a parallel between the MNB and brain NBs. Thus, the MNB has a number of properties distinct from other nerve cord NBs in that it is not part of a neural/epidermal equivalence group and does not utilize the Hunchback>Krüppel>Pdm>Cas cascade (Isshiki et al., 2001). Similarly, it is unusual that VUM5,6 require *Notch* function, as *Notch* signaling inhibited MP1,3 and MP4 neurogenesis. Consistent with the genetic data, *P[12xSu(H)bs-lacZ]* expression is restricted to MP5,6 and the MNB. This suggests that the different responses to *Notch* signaling might reflect anterior-posterior location. However, there might also be differences with respect to cell type, because *sim-Gal4 UAS-Su(H).VP16* embryos have expanded MNB-like cells, but the MP5,6 cells were not expanded. One potential model involves successive waves of signaling, by *Notch* or other signaling molecules, to generate the MNB, MP5,6 and MG, similar to what happens during development of the *Drosophila* retina (e.g. Doroquez and Rebay, 2006). Bossing and Brand have proposed an equivalence group in which *Notch* signaling would inhibit cells from becoming a MNB, and instead promote the VUM cell fate (Bossing and Brand, 2006). However, our *Dl* mutant and *Su(H).VP16* misexpression data indicate that *Notch* signaling promotes, not inhibits, MNB formation. Another view is that the presence of PMG is required for MP5,6 and MNB formation, and that the absence of PMG in *Dl* mutants also results in the loss of the neural precursors. In summary, alterations in *Notch* signaling have revealed its requirement in the formation of MP5,6 and the MNB, but additional work will be required for mechanistic insight.

## *Notch* signaling and *numb* generate asymmetric midline neuronal cell fates

Asymmetric neuronal cell fates of MP3-6 progeny are determined by Numb and Spdo asymmetric localization in one of the two daughter cells (Fig. 8), similar to asymmetric cell fate determination of the non-midline MP2 cell and GMCs (O'Connor-Giles and Skeath, 2003; Spana and Doe, 1996; Spana et al., 1995). In the H-cell sib and iVUMs, Numb is absent, and *Notch* signaling, in combination with cortical Spdo, activates H-cell sib- and iVUM-specific gene expression and represses H-cell and mVUM gene expression. Genes that are expressed in both siblings are not dependent on *Notch* signaling. The MP1 progeny are identical by gene expression and morphological criteria. Numb is present in both MP1 neurons, but the significance of this is unclear because MP1 gene expression and morphology were unaffected in *numb* mutants; nor were defects observed in *Dl* mutants. This suggests that *Notch* signaling does not influence MP1 development.

Another difference between MP1 and the other MPs is that MP1 divides perpendicular to the apical-basal axis, whereas MP3-6 rotate their spindles during cell division along the apical-basal axis. The basal cell is always the Numb$^+$ cell, which is the *Notch*-independent H-cell or mVUM. The orientations of the divisions might aid in positioning the cells towards their final locations in the CNS. In the mature CNS, the iVUMs are apical to the mVUMs, and during MP divisions the iVUM is the more apical sibling. In the case of the MP1s, it might be important that both cells are in the same position along the basal/apical axis.

Kuwada and Goodman examined the development of grasshopper MP3 (Kuwada and Goodman, 1985). Their data suggested a model in which the two MP3 neurons are born equivalent with an H-cell sib dominant fate, and, within 5 hours, signaling between the two cells generates different fates. These

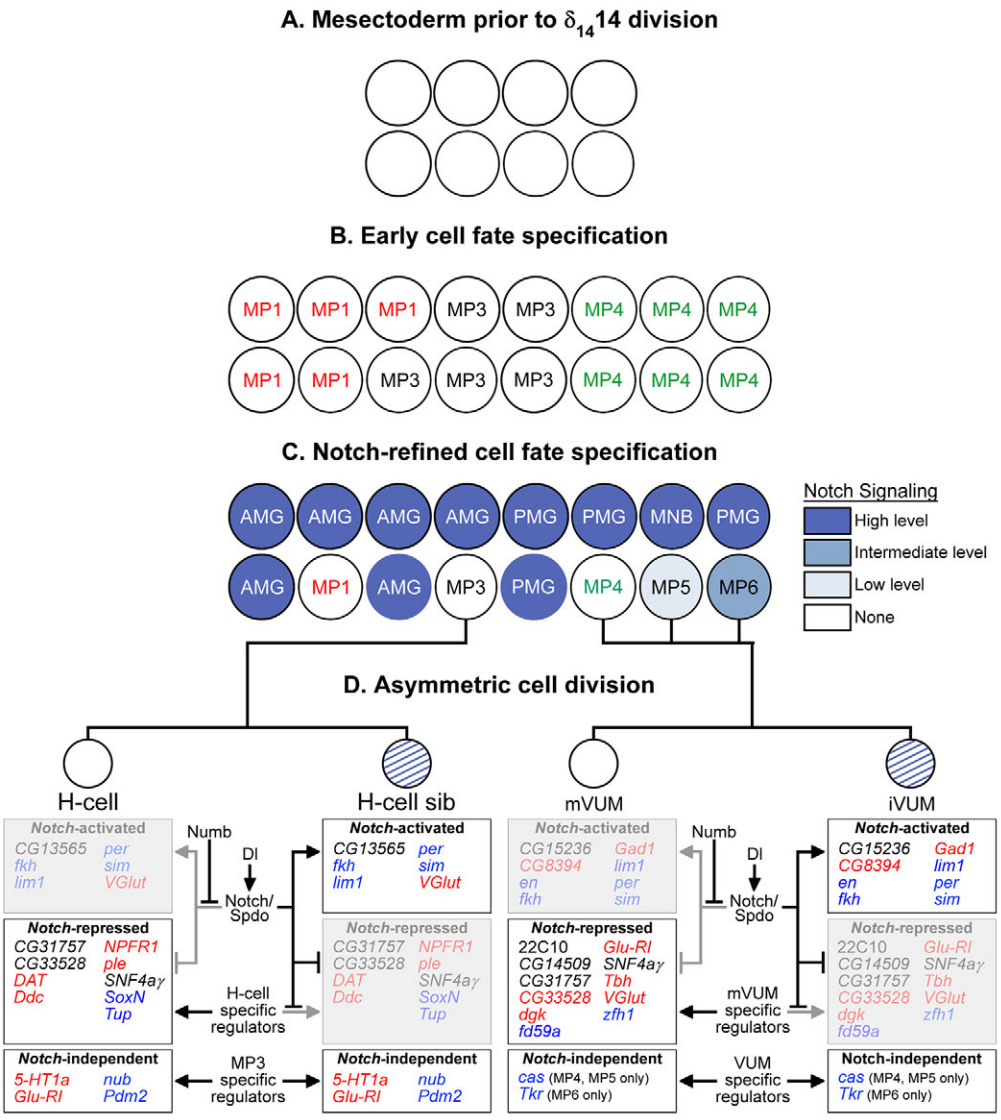


**Fig. 8. Model of *Notch* regulation of midline cell fate in *Drosophila*.** (**A**) Mesectodermal cells meet at the ventral midline before the stage 8 $\delta_{14}$14 division. Little is known regarding influences on midline cell development at this stage. (**B**) After the stage 8 division, but before *Notch* signaling, the 16 midline cells can be considered as three equivalent groups of cells: MP1s, MP3s and MP4s. (**C**) After *Notch* signaling, the 16 cells acquire specific fates, and differ in their levels of *Notch* signaling as indicated by the expression of *Su(H)-lacZ* reporter. For simplicity, midline cells are shown as paired cells along the anterior-posterior axis. The precise anterior-posterior and left-right positions of individual cells are unknown, except that AMG, MP1 and MP3 tend to reside in the anterior half, and PMG, MP5, MP6 and MNB in the posterior half. Different shades of blue indicate relative levels of *Notch* signaling. (**D**) Asymmetric cell division. *Notch* signaling is required for MP3-6 asymmetric cell fates. *Notch* signaling is active (blue diagonals) in H-cell sib and iVUMs, and inhibited in H-cell and mVUMs. Assayed genes expressed in the MP3 and VUM lineages are shown below each neuron: bold text indicates expression, whereas the light, shaded text indicates repression. Genes are categorized as either *Notch*-activated, *Notch*-repressed or *Notch*-independent. Functional classes of genes are color-coded: transcription factors (blue), neural function genes (red) and others (black).

data appear inconsistent with the *Drosophila* results, as the *Drosophila* MP3 neurons asymmetrically localize Numb and are inherently different at birth. However, it is important to recognize that the grasshopper and *Drosophila* results are based on different types of experiments (genetic versus experimental ablation), and the grasshopper data might be revealing additional levels of regulation or different mechanisms for generating cell fates.

## Towards a molecular basis for neuronal and glial cell fate determination

Nearly 300 genes are known to be expressed in the developing *Drosophila* CNS midline cells, and many have been mapped at the single-cell level by confocal microscopy. The work described here examined the role of *Notch* signaling in the expression of 37 MG- and neuronal-expressed genes (Fig. 8). Molecular analysis can now be carried out on these genes to identify direct targets of *Notch* action. Additional studies are also beginning to identify transcription factors that regulate the *Notch*-independent neuronal pathways (our unpublished results). The large number of genes identified, in combination with the utility of *Drosophila* molecular and genetic tools, will facilitate a detailed understanding of the regulatory pathways controlling midline neurogenesis and gliogenesis.

We thank Amaris Guardiola, Catarina Homem, Joe Kearney, Tony Perdue, Nasser Rusan and Ferrin Wheeler for valuable advice and assistance; Stephanie Freer for investigation of larval phenotypes; and Joe Pearson for helpful comments on the manuscript. We are grateful to Spyros Artavanis-Tsakonas, Nipam Patel and Francois Schweisguth for contributing antibodies and fly stocks; and are particularly appreciative of the endless advice and supplies from Jim Skeath and Beth Wilson. We also thank the Developmental Studies Hybridoma Bank for monoclonal antibodies and the Bloomington *Drosophila* Stock Center for fly stocks. This work was supported by NIH grant R37 RD25251 to S.T.C., an NRSA postdoctoral fellowship to S.R.W., and UNC Developmental Biology NIH training grant support to S.B.S.

### Supplementary material

Supplementary material for this article is available at http://dev.biologists.org/cgi/content/full/135/18/3071/DC1

### References

**Abramoff, M. D., Magelhaes, P. J. and Ram, S. J.** (2004). Image processing with ImageJ. *Biophotonics Int.* **11**, 36-42.
**Almeida, M. S. and Bray, S. J.** (2005). Regulation of post-embryonic neuroblasts by Drosophila Grainyhead. *Mech. Dev.* **122**, 1282-1293.

**Bate, C. M. and Grunewald, E. B.** (1981). Embryogenesis of an insect nervous system II: a second class of neuron precursor cells and the origin of the intersegmental connectives. *J. Embryol. Exp. Morphol.* **61**, 317-330.
**Bossing, T. and Technau, G. M.** (1994). The fate of the CNS midline progenitors in Drosophila as revealed by a new method for single cell labelling. *Development* **120**, 1895-1906.
**Bossing, T. and Brand, A. H.** (2006). Determination of cell fate along the anteroposterior axis of the Drosophila ventral midline. *Development* **133**, 1001-1012.
**Brand, A.** (1995). GFP in Drosophila. *Trends Genet.* **11**, 324-325.
**Broihier, H. T. and Skeath, J. B.** (2002). Drosophila homeodomain protein dHb9 directs neuronal fate via crossrepressive and cell-nonautonomous mechanisms. *Neuron* **35**, 39-50.
**Campos-Ortega, J. A.** (1993). Early neurogenesis in *Drosophila melanogaster*. In *The Development of Drosophila melanogaster*, vol. 2 (ed. M. Bate and A. M. Arias), pp. 1091-1129. Cold Spring Harbor, NY: Cold Spring Harbor Laboratory Press.
**Crews, S. T.** (2003). Drosophila bHLH-PAS developmental regulatory proteins. In *PAS Proteins: Regulators and Sensors of Development and Physiology* (ed. S. T. Crews), pp. 69-108. New York: Kluwer Academic Publishers.
**Doroquez, D. B. and Rebay, I.** (2006). Signal integration during development: mechanisms of EGFR and Notch pathway function and cross-talk. *Crit. Rev. Biochem. Mol. Biol.* **41**, 339-385.
**Foe, V. E.** (1989). Mitotic domains reveal early commitment of cells in Drosophila embryos. *Development* **107**, 1-22.
**Furriols, M. and Bray, S.** (2001). A model Notch response element detects Suppressor of Hairless-dependent molecular switch. *Curr. Biol.* **11**, 60-64.
**Gaiano, N., Nye, J. S. and Fishell, G.** (2000). Radial glial identity is promoted by Notch1 signaling in the murine forebrain. *Neuron* **26**, 395-404.
**Go, M. J., Eastman, D. S. and Artavanis-Tsakonas, S.** (1998). Cell proliferation control by Notch signaling in Drosophila development. *Development* **125**, 2031-2040.
**Goodman, C. S., Bate, M. and Spitzer, N. C.** (1981). Embryonic development of identified neurons: origin and transformation of the H cell. *J. Neurosci.* **1**, 94-102.
**Hutterer, A. and Knoblich, J. A.** (2005). Numb and alpha-Adaptin regulate Sanpodo endocytosis to specify cell fate in Drosophila external sensory organs. *EMBO Rep.* **6**, 836-842.
**Isshiki, T., Pearson, B., Holbrook, S. and Doe, C. Q.** (2001). Drosophila neuroblasts sequentially express transcription factors which specify the temporal identity of their neuronal progeny. *Cell* **106**, 511-521.
**Jacobs, J. R.** (2000). The midline glia of Drosophila: a molecular genetic model for the developmental functions of glia. *Prog. Neurobiol.* **62**, 475-508.
**Jia, X. X. and Siegler, M. V.** (2002). Midline lineages in grasshopper produce neuronal siblings with asymmetric expression of Engrailed. *Development* **129**, 5181-5193.
**Kambadur, R., Koizumi, K., Stivers, C., Nagle, J., Poole, S. J. and Odenwald, W. F.** (1998). Regulation of POU genes by castor and hunchback establishes layered compartments in the Drosophila CNS. *Genes Dev.* **12**, 246-260.
**Kearney, J. B., Wheeler, S. R., Estes, P., Parente, B. and Crews, S. T.** (2004). Gene expression profiling of the developing Drosophila CNS midline cells. *Dev. Biol.* **275**, 473-492.
**Kidd, S., Lieber, T. and Young, M. W.** (1998). Ligand-induced cleavage and regulation of nuclear entry of Notch in Drosophila melanogaster embryos. *Genes Dev.* **12**, 3728-3740.
**Klambt, C., Jacobs, J. R. and Goodman, C. S.** (1991). The midline of the Drosophila central nervous system: a model for the genetic analysis of cell fate, cell migration, and growth cone guidance. *Cell* **64**, 801-815.
**Kosman, D., Small, S. and Reinitz, J.** (1998). Rapid preparation of a panel of polyclonal antibodies to Drosophila segmentation proteins. *Dev. Genes Evol.* **208**, 290-294.
**Kuwada, J. Y. and Goodman, C. S.** (1985). Neuronal determination during embryonic development of the grasshopper nervous system. *Dev. Biol.* **110**, 114-126.
**Lee, C. Y., Andersen, R. O., Cabernard, C., Manning, L., Tran, K. D., Lanskey, M. J., Bashirullah, A. and Doe, C. Q.** (2006). Drosophila Aurora-A kinase inhibits neuroblast self-renewal by regulating aPKC/Numb cortical polarity and spindle orientation. *Genes Dev.* **20**, 3464-3474.
**Liu, X., Zwiebel, L. J., Hinton, D., Benzer, S., Hall, J. C. and Rosbash, M.** (1992). The period gene encodes a predominantly nuclear protein in adult Drosophila. *J. Neurosci.* **12**, 2735-2744.
**Ma, Y., Certel, K., Gao, Y., Niemitz, E., Mosher, J., Mukherjee, A., Mutsuddi, M., Huseinovic, N., Crews, S. T., Johnson, W. A. et al.** (2000). Functional interactions between Drosophila bHLH/PAS, Sox, and POU transcription factors regulate CNS midline expression of the slit gene. *J. Neurosci.* **20**, 4596-4605.
**Menne, T. V. and Klambt, C.** (1994). The formation of commissures in the Drosophila CNS depends on the midline cells and on the Notch gene. *Development* **120**, 123-133.
**Morrison, S. J., Perez, S. E., Qiao, Z., Verdi, J. M., Hicks, C., Weinmaster, G. and Anderson, D. J.** (2000). Transient Notch activation initiates an irreversible switch from neurogenesis to gliogenesis by neural crest stem cells. *Cell* **101**, 499-510.
**O'Connor-Giles, K. M. and Skeath, J. B.** (2003). Numb inhibits membrane localization of Sanpodo, a four-pass transmembrane protein, to promote asymmetric divisions in Drosophila. *Dev. Cell* **5**, 231-243.
**Patel, N. H., Martin-Blanco, E., Coleman, K. G., Poole, S. J., Ellis, M. C., Kornberg, T. B. and Goodman, C. S.** (1989). Expression of engrailed proteins in arthropods, annelids, and chordates. *Cell* **58**, 955-968.
**Schmid, A., Chiba, A. and Doe, C. Q.** (1999). Clonal analysis of Drosophila embryonic neuroblasts: neural cell types, axon projections and muscle targets. *Development* **126**, 4653-4689.
**Skeath, J. B. and Doe, C. Q.** (1998). Sanpodo and Notch act in opposition to Numb to distinguish sibling neuron fates in the Drosophila CNS. *Development* **125**, 1857-1865.
**Spana, E. P. and Doe, C. Q.** (1996). Numb antagonizes Notch signaling to specify sibling neuron cell fates. *Neuron* **17**, 21-26.
**Spana, E. P., Kopczynski, C., Goodman, C. S. and Doe, C. Q.** (1995). Asymmetric localization of numb autonomously determines sibling neuron identity in the Drosophila CNS. *Development* **121**, 3489-3494.
**Thomas, J. B., Crews, S. T. and Goodman, C. S.** (1988). Molecular genetics of the *single-minded* locus: a gene involved in the development of the Drosophila nervous system. *Cell* **52**, 133-141.
**Truman, J. W., Schuppe, H., Shepherd, D. and Williams, D. W.** (2004). Developmental architecture of adult-specific lineages in the ventral CNS of Drosophila. *Development* **131**, 5167-5184.
**Udolph, G., Rath, P. and Chia, W.** (2001). A requirement for Notch in the genesis of a subset of glial cells in the Drosophila embryonic central nervous system which arise through asymmetric divisions. *Development* **128**, 1457-1466.
**Uemura, T., Shepherd, S., Ackerman, L., Jan, L. Y. and Jan, Y. N.** (1989). numb, a gene required in determination of cell fate during sensory organ formation in Drosophila embryos. *Cell* **58**, 349-360.
**Wang, H., Ouyang, Y., Somers, W. G., Chia, W. and Lu, B.** (2007). Polo inhibits progenitor self-renewal and regulates Numb asymmetry by phosphorylating Pon. *Nature* **449**, 96-100.
**Wang, S., Younger-Shepherd, S., Jan, L. Y. and Jan, Y. N.** (1997). Only a subset of the binary cell fate decisions mediated by Numb/Notch signaling in Drosophila sensory organ lineage requires Suppressor of Hairless. *Development* **124**, 4435-4446.
**Ward, E. J. and Skeath, J. B.** (2000). Characterization of a novel subset of cardiac cells and their progenitors in the Drosophila embryo. *Development* **127**, 4959-4969.
**Ward, M. P., Mosher, J. T. and Crews, S. T.** (1998). Regulation of bHLH-PAS protein subcellular localization during Drosophila embryogenesis. *Development* **125**, 1599-1608.
**Wech, I., Bray, S., Delidakis, C. and Preiss, A.** (1999). Distinct expression patterns of different enhancer of split bHLH genes during embryogenesis of Drosophila melanogaster. *Dev. Genes Evol.* **209**, 370-375.
**Wharton, K. A., Jr, Franks, R. G., Kasai, Y. and Crews, S. T.** (1994). Control of CNS midline transcription by asymmetric E-box-like elements: similarity to xenobiotic responsive regulation. *Development* **120**, 3563-3569.
**Wheeler, S. R., Kearney, J. B., Guardiola, A. R. and Crews, S. T.** (2006). Single-cell mapping of neural and glial gene expression in the developing Drosophila CNS midline cells. *Dev. Biol.* **294**, 509-524.
**Xiao, H., Hrdlicka, L. A. and Nambu, J. R.** (1996). Alternate functions of the single-minded and rhomboid genes in development of the Drosophila ventral neuroectoderm. *Mech. Dev.* **58**, 65-74.